



PERGAMON

Available online at www.sciencedirect.com

SCIENCE @ DIRECT®

Applied
Radiation and
Isotopes

Applied Radiation and Isotopes 58 (2003) 245–261

www.elsevier.com/locate/apradiso

Excited levels in ^{149}Pm from the decay of ^{149}Nd

I.M.M.A. Medeiros^a, C.B. Zamboni^a, F.A. Genezini^{a,b}, J.A.G. de Medeiros^{a,b},
M.T.F. da Cruz^{c,*}, J.Y. Zevallos-Chávez^c

^a Instituto de Pesquisas Energéticas e Nucleares, IPEN/CNEN-SP, Rua do Matão, Travessa, R 400, São Paulo, 05508-900, Brazil

^b Universidade Santo Amaro, UNISA-SP, São Paulo, Brazil

^c Instituto de Física, Universidade de São Paulo - IFUSP, Lab. do Acelerador Linear, C.P. 66318, São Paulo SP 05315-970, Brazil

Received 19 August 2002; received in revised form 08 October 2002; accepted 10 October 2002

Abstract

The level structure of ^{149}Pm has been investigated by studying the gamma rays emitted following the β^- decay of ^{149}Nd ($T_{1/2} = 1.7$ h). The singles and the $\gamma\gamma$ coincidence spectra were taken using HPGe detectors with high energy resolution. The energy and relative intensities of 198 gamma rays have been determined, 45 for the first time and several multiplets were resolved using bidimensional data analysis. A decay scheme with 51 levels has been proposed. This includes 6 new levels, at 1407, 1368, 1364, 1329, 1293 and 1181 keV. The present results permitted assignments of spin and parity for a number of these levels.

© 2003 Elsevier Science Ltd. All rights reserved.

Keywords: Beta decay; Gamma spectroscopy; Energy; Neodimium

1. Introduction

The level structure of the Promethium ($Z=61$), Europium ($Z=63$) and Terbium ($Z=65$) nuclei have been investigated intensely in the last two decades, indicating shape transitions from spherical to deformed as the neutron number increases from 86 to 90. While nuclei like ^{151}Eu and ^{153}Tb have been described primarily through spherical approaches (Chen and Arns, 1965; Schneider et al., 1979) the isotones, with $N=90$, ^{151}Pm , ^{153}Eu and ^{155}Tb have been interpreted in terms of the particle deformed-core approaches (Hartley et al., 1998). But, there is no conclusive theoretical description involving the low-energy excited levels in ^{149}Pm because the experimental results are few and particularly the data from beta decay of ^{149}Nd are not consistent. Basically, the results of two studies performed by Schneider et al. (1979) and more recently by Hideki et al. (1986), established the features of the excited levels in ^{149}Pm . In the work performed by Schneider et al.

(1979) the γ -ray spectrum, in singles and coincidence experiments, was examined using Ge(Li) detector. According to this work 214 γ transitions were attributed to this decay, with 201 placed in 42 energy levels. The measurement performed by Hideki et al. (1986) involving γ spectroscopy and $\gamma\gamma$ angular correlation of the most intense cascades, suggests a decay scheme with 199 γ transitions arranged in 40 energy levels, but no experimental uncertainty was reported for γ energy measurements and the intensity values for these γ transitions were not determined. According to the last compilation by Firestone (1996) this isotope has been studied by several different nuclear reactions, such as, ^{148}Nd ($^3\text{He},d$) and ^{148}Nd (α,t) (Straume et al., 1976), ^{150}Sm ($\text{pol } t,\alpha$) and ^{150}Sm ($d,^3\text{He}$) (Firestone, 1996) but some controversies, regarding the presence and placement, of several γ transitions in the level scheme remain unsolved when beta decay data are compared with these nuclear reactions studies. Besides, a number of γ transitions must be confirmed and nuclear parameters such as energy, spin, parity and branching ratio of excited levels as well as energy and intensity of gamma transition in this decay scheme still need verification.

*Corresponding author.

E-mail address: tiago@if.usp.br (M.T.F. da Cruz).

An attempt to propose a well established β^- decay scheme of ^{149}Nd motivated us to performed an investigation of excited levels in ^{149}Pm by means of γ -ray spectroscopy and $\gamma\gamma$ coincidence measurements. These measurements were performed at Instituto de Pesquisas Energéticas e Nucleares, São Paulo (IPEN) and Instituto de Física da Universidade de São Paulo, São Paulo (IFUSP) facilities.

2. Experimental procedure

The sources of ^{149}Nd were generated by thermal neutron irradiation of Nd_2O_3 (enriched to 94% by the ^{148}Nd isotope). About 10 mg of ^{148}Nd were irradiated for 5 min in the IEA-R1 reactor at a neutron flux of 10^{12} neutrons $\text{cm}^{-2}\text{s}^{-1}$. The γ -ray spectra from ^{149}Nd were recorded through five successive half-lives using a HPGe coaxial detector of 75 cm^3 active volume and an Ortec 671 amplifier, in pile-up rejection mode. The background radiation was reduced by employing the iron shield described by Medeiros et al. (2001).

Gamma–gamma coincidence spectra were measured using a multidetector acquisition system (Barg et al., 1997), with two 90 cm^3 HPGe detectors (FWHM < 1.82-keV at 1.32 MeV of ^{60}Co). The energy calibration and the relative efficiencies of these detectors were done using the standard gamma rays of ^{60}Co , ^{109}Cd , ^{133}Ba , ^{137}Cs and ^{152}Eu .

The direct γ -ray spectrum from about 30 keV to 1.6 MeV was analyzed using the same procedure described by Camargo et al. (1998) and the coincidence data, for the same energy range, have been analyzed using the BIDIM program (Guimarães Filho, 1998).

3. Experimental results

In this experiment we have observed 198 gamma rays belonging to the β^- decay of ^{149}Nd . Forty five transitions at 26, 34, 39, 44, 58, 67, 69, 73, 77, 80, 90, 93, 171, 224, 239, 290, 332, 372, 414, 435, 441, 591, 653, 665, 727, 736, 772, 795, 806, 835, 839, 859, 933, 976, 1016, 1041, 1120, 1171, 1180, 1207, 1238, 1293, 1368, 1401 and 1407 keV were observed for the first time. Table 1 shows the energy, relative intensity and the placement, when it was possible. Figs. 1–10 show the singles gamma ray spectrum recorded during 200 h of live time counting.

When our energies and intensity values of the γ transitions were confronted with data from the last study performed by Schneider et al. (1979) we noticed that most of the results were in agreement with them, but some controversies were also observed and these will be discussed now. First, no evidence was found which confirmed the existence the γ transitions at 112, 273, 329,

399, 510, 513, 537, 564, 559, 607, 618, 657, 672, 704, 743, 818, 850, 854, 878, 908, 915, 920, 930, 936, 939, 972, 987, 1136, 1142, 1150, 1156, 1176, 1190, 1226, 1285, 1298, 1307, 1312, 1357, 1381, 1454 and 1569 keV proposed only by them; a research was made in our single and coincidence data and although we have high statistics in both measurements no evidences involving these transitions were found. About the doublet at 75 keV (deexcitations $462.2 \rightarrow 387.6$ keV and $188.6 \rightarrow 114.3$ keV according to the authors), suggested only by Schneider et al. (1979), it was not solved in our single analyses and our coincidence data strongly agree that this peak can be positioned depopulating the level at 462 keV (see Table 2), but the existence of 75–349 and 75–583 keV coincidences is only possible by assuming that the peak at 75 keV is a doublet, in this case positioned at: $188 \rightarrow 114$ keV, so in agreement with them. However, the doublets at: 357.02 and 358.49 keV; 443.56 and 443.70 keV; 556.83 and 558.01 keV; 671.64 and 673.59 keV; 864.89 and 864.90 keV; 1125.31 and 1126.61 keV suggested by them were found to be singlets, according to the present study.

We also confront our energy and intensity values of the γ transitions with the compilation performed by Firestone (1996) and we are proposing that the photopeaks at: 59, 240, 433, 728, 793, 1041 and 1171 keV presented as singlets in this compilation are, in fact, doublets at: 59 keV [58.5 and 59.8 keV]; 240 keV [238.6 and 240.5 keV]; 433 keV [432.8 and 434.9 keV]; 728 keV [726.8 and 727.2 keV]; 793 keV [793.2 and 794.5 keV], 1041 keV [1040.7 and 1042.3 keV] and 1171 keV [1170.9 and 1172.8 keV] according to our singles and coincidence data.

From the analysis of the energy determinations, the transitions at 318, 449, 750, 809 and 992 keV reported by one previous experiment performed by Szuëcs et al. (1985) they were also assigned in the present scheme proposal of ^{149}Nd decay.

In the present $\gamma\gamma$ coincidence experiment the search was made for 91 gates. A summary of the observed coincidences is shown in Table 2. Our coincidence data and energy-sum analysis led us to place 181 γ -rays in the decay scheme, 30 of them were observed for the first time. Most the total set of transitions positioned agree with the placements suggested in early studies (Schneider et al., 1979; Hideki et al., 1986). The placements are in disagreement for only three γ -rays. It is the case of the doublet at 634.9 and 636.0 and the transition at 776 keV. According to Schneider et al. (1979) and Hideki et al. (1986) this doublet has been attributed to the de-excitation from 934 to 750 keV levels, respectively but, when we analyze the gate at $635 + 636$ keV (see Table 2) the doublet must be placed at: $751 \rightarrow 114$ keV (635 keV) and $636 \rightarrow 0$ keV (636 keV) to agree with our coincidence results. As for the transition at 776 keV, it has been previously placed in the ^{149}Nd decay scheme

Table 1

Energy, relative intensity and placement of γ -ray following the beta decay of ^{149}Nd . The values published previously by Schneider et al. (1979) were included for comparison

This work Energy(keV)	$I_{\gamma}(\%)$	Schneider et al. (1979) Energy(keV)	$I_{\gamma}(\%)$	This work $E_i \rightarrow E_f$ (keV \rightarrow keV)
—	—	22.68 (3) ^a	0.21 (6)	—
26.394 (22)	—	—	—	—
30.077 (26)	—	29.94 (2) ^a	0.67 (17)	270.2069(15) \rightarrow 240.3946 (19)
33.964 (16)	—	—	—	—
—	—	36.71 (10) ^a	0.70 (30)	—
39.065 (9)	—	—	—	—
44.341 (14)	—	—	—	—
58.526 (11)	54.7 (9)	—	—	—
59.652 (8)	76.6 (13)	58.85 (3) ^a	50.00(80)	270.2069 (15) \rightarrow 211.3624 (15)
65.792 (8)	3.4 (4)	65.24 (10) ^a	0.60 (20)	462.349 (3) \rightarrow 396.8556 (23)
—	—	65.42 (10) ^a	1.20 (40)	—
67.20 (19)	1.7 (4)	—	—	—
69.510 (21)	2.5 (3)	—	—	270.2069 (15) \rightarrow 211.3624 (15)
72.753 (12)	23.0 (5)	—	—	—
—	—	74.33 (3) ^a	42.70 (93)	—
74.932 (4)	124.5 (10)	74.62 (4) ^a	38.10 (58)	462.349 (3) \rightarrow 387.609 (4)
—	—	75.63 (9)	8.80 (80)	—
77.097 (10)	23.5 (5)	—	—	—
80.305 (10)	17.4 (3)	—	—	—
90.12 (5)	1.99 (11)	—	—	515.796 (4) \rightarrow 425.2798 (22)
92.89 (3)	2.16 (13)	—	—	—
—	—	94.88 (10)	1.60 (50)	—
96.3 (3)	1.8 (11)	96.90 (16) ^a	1.30 (50)	654.9478 (23) \rightarrow 556.233 (4)
97.354 (17)	44.14 (4)	96.99 (2) ^a	55.60 (42)	211.3624 (15) \rightarrow 114.3534 (15)
108.189 (14)	5.4 (4)	107.78 (12)	3.30 (60)	654.9478 (23) \rightarrow 547.076 (6)
—	—	112.52 (4)	4.60 (60)	—
114.066(11)	651.3 (7)	114.30 (2)	734.60 (529)	114.3534 (15) \rightarrow 0
117.088 (8)	8.09 (7)	116.78 (27)	4.2 (12)	654.9478 (23) \rightarrow 537.9789 (20)
122.689 (8)	8.26 (4)	122.40 (6)	9.9 (60)	537.9789 (20) \rightarrow 415.559 (5)
126.513 (17)	3.03 (23)	126.60 (8)	4.3 (30)	396.8556 (23) \rightarrow 270.2069 (15)
137.288 (20)	5.14 (4)	137.10 (7)	2.40 (20)	425.2798 (22) \rightarrow 288.2274 (21)
139.357 (7)	23.3 (8)	139.20 (3)	19.6 (90)	654.9458 (23) \rightarrow 515.796 (4)
140.93 (5)	5.0 (3)	141.06 (7)	1.50 (10)	537.9789 (20) \rightarrow 396.8556 (23)
154.74 (6)	4.5 (3)	155.12 (10) ^a	1.3 (60)	425.2798 (22) \rightarrow 270.2069 (15)
156.048 (3)	230.7 (5)	155.86 (2) ^a	228.8 (85)	270.2069 (15) \rightarrow 114.3534 (15)
171.17 (10)	1.24 (22)	—	—	—
175.33 (8)	1.44 (4)	176.25 (4) ^a	1.9 (40)	387.609 (4) \rightarrow 211.3624 (15)
177.905 (13)	5.9 (5)	177.73 (5) ^a	6.0 (60)	537.9789 (20) \rightarrow 360.139 (5)
185.617 (9)	5.79 (12)	185.47 (5)	4.00 (20)	396.8556 (23) \rightarrow 211.3624 (15)
188.7832 (23)	69.9 (3)	188.64 (2)	69.5 (31)	188.6796 (17) \rightarrow 0
192.171 (3)	22.07 (15)	192.02 (3)	22.00 (70)	462.349 (3) \rightarrow 270.2069 (15)
197.75 (8)	3.1 (3)	197.80 (6) ^a	1.90 (20)	556.233 (4) \rightarrow 360.139 (5)
199.066 (5)	55.8 (5)	198.93 (2) ^a	53.7 (17)	3987.609 (4) \rightarrow 188.6796 (17)
208.3210 (21)	105.26 (9)	208.14 (3)	98.3 (40)	396.8556 (23) \rightarrow 188.6796 (17)
211.4403 (20)	1000 (18)	211.32 (2)	1000 (403)	211.3624 (15) \rightarrow 0
213.9414 (20)	11.59 (7)	213.97 (7)	15.4 (10)	425.2798 (22) \rightarrow 211.3624 (15)
224.49 (6)	0.92 (9)	—	—	1181.18 (6) \rightarrow 956.83 (7)
227.072 (9)	5.44 (6)	226.85 (4)	6.30 (20)	415.559 (5) \rightarrow 188.6796 (17)
229.630 (3)	17.71 (9)	229.58 (2)	18.60 (50)	654.9478 (23) \rightarrow 425.2798 (22)
238.611 (3)	34.32 (11)	—	—	—
240.4660 (18)	122.89 (22)	240.23 (2)	151.8 (60)	240.3946 (19) \rightarrow 0
244.89 (15)	3.6 (12)	245.49 (7) ^a	8.5 (40)	515.796 (4) \rightarrow 270.2069 (15)
245.847 (21)	36.18 (15)	245.71 (2) ^a	31.4 (80)	360.139 (5) \rightarrow 114.3534 (15)
250.82 (3)	1.06 (27)	250.83 (4)	1.30 (10)	462.349 (3) \rightarrow 211.3624 (15)
254.783 (15)	3.69 (12)	254.25 (3)	3.30 (10)	651.132 (6) \rightarrow 396.8556 (23)

Table 1 (continued)

This work Energy(keV)	I_{γ} (%)	Schneider et al. (1979) Energy(keV)	I_{γ} (%)	This work $E_i \rightarrow E_f$ (keV \rightarrow keV)
258.144 (3)	15.73 (20)	258.08 (3)	14.5 (40)	654.9458 (23) \rightarrow 396.8556 (23)
267.7873 (16)	218.11 (8)	267.70 (2)	232.9 (59)	537.9789 (20) \rightarrow 270.2069 (15)
270.2449 (16)	385.13 (11)	270.17 (2)	413 (105)	270.2069 (15) \rightarrow 0
—	—	273.25 (5) ^a	6.8 (30)	—
—	—	273.55 (8) ^a	3.20 (15)	—
275.469 (5)	15.29 (8)	275.42 (2)	25.10 (60)	515.796 (4) \rightarrow 240.3946 (19)
276.89 (8)	10.09 (8)	276.96 (4)	13.2 (40)	547.076 (6) \rightarrow 270.2069 (15)
281.958 (14)	6.88 (21)	282.40 (9) ^a	0.65 (25)	744.575 (6) \rightarrow 462.349 (3)
282.5292 (25)	20.71 (12)	282.46 (2) ^a	23.8 (60)	396.8556 (23) \rightarrow 114.3534 (15)
286.034 (4)	15.31 (13)	287.76 (12) ^a	0.50 (20)	556.233 (4) \rightarrow 270.2069 (15)
288.2516 (25)	23.31 (14)	288.20 (2) ^a	26.7 (70)	288.2274 (21) \rightarrow 0
290.374 (20)	2.43 (6)	—	—	651.132 (6) \rightarrow 360.139 (5)
294.969 (7)	33.3 (7)	294.79 (2)	22.0 (60)	654.9478 (23) \rightarrow 360.139 (5)
301.097 (9)	12.4 (4)	301.11 (3)	14.0 (40)	415.559 (5) \rightarrow 114.3534 (15)
311.059 (3)	17.6 (3)	310.97 (3)	19.7 (50)	425.2798 (22) \rightarrow 114.3534 (15)
318.02 (12)	6.15 (18)	318.2 (3)	0.33 (17)	556.233 (4) \rightarrow 240.3946 (19)
326.6331 (17)	165.89 (16)	326.54 (3)	175.9 (43)	537.9789 (20) \rightarrow 211.3624 (15)
—	—	329.13 (7) ^a	0.80 (40)	—
332.167 (18)	0.68 (4)	—	—	1363.85 (4) \rightarrow 1031.75 (4)
343.12 (5)	1.4 (4)	342.95 (18) ^a	3.2 (70)	767.482 (12) \rightarrow 425.2798 (22)
347.654 (19)	23.8 (3)	347.86 (3)	6.20 (20)	744.575 (6) \rightarrow 396.8556 (23)
349.365 (4)	85.40 (10)	349.22 (3)	53.1 (14)	537.9789 (20) \rightarrow 188.6796 (17)
351.632 (3)	45.1 (6)	352.79 (4)	2.10 (10)	—
357.111 (22)	2.82 (14)	357.02 (4)	4.80 (10)	744.575 (6) \rightarrow 787.609 (4)
—	—	358.49 (1)	0.40 (20)	—
359.889 (20)	5.93 (15)	360.04 (4)	5.90 (20)	360.139 (5) \rightarrow 0
361.76 (3)	5.14 (13)	361.40 (20) ^a	0.25 (10)	721.929 (26) \rightarrow 360.139 (5)
366.682 (3)	18.58 (17)	366.62 (4)	20.9 (60)	654.9478 (23) \rightarrow 288.2274 (21)
371.92 (6)	0.86 (10)	—	—	1328.79 (9) \rightarrow 956.83 (7)
376.69 (10)	0.43 (11)	376.90 (2) ^a	0.30 (15)	1031.75 (4) \rightarrow 654.9478 (23)
380.962 (22)	1.63 (4)	380.66 (5)	2.00 (10)	651.132 (6) \rightarrow 270.2069 (15)
384.703 (4)	9.37 (5)	384.67 (4)	10.3 (30)	654.9378 (23) \rightarrow 270.2069 (15)
390.65 (16)	0.21 (3)	390.96 (7) ^a	0.30 (10)	1141.67 (4) \rightarrow 750.491 (15)
396.878 (12)	2.98 (4)	396.75 (5)	2.80 (10)	396.8556 (23) \rightarrow 0
—	—	399.14 (9) ^a	0.56 (22)	—
413.693 (15)	0.67 (5)	—	—	1049.655 (24) \rightarrow 635.983 (25)
423.5600 (20)	252.5 (4)	423.54 (4)	287 (151)	537.9789 (20) \rightarrow 114.3534 (15)
425.86 (11)	25.5 (3)	425.33 (6)	10.5 (40)	425.2798 (22) \rightarrow 0
432.76 (7)	0.14 (4)	432.81 (7) ^a	0.54 (25)	547.076 (6) \rightarrow 114.3534 (15)
434.90 (7)	0.14 (4)	—	—	1156.971 (8) \rightarrow 721.929 (26)
439.11 (7)	1.45 (14)	439.65 (14) ^a	1.4 (60)	651.132 (6) \rightarrow 211.3624 (15)
441.47 (13)	1.22 (10)	—	—	956.83 (7) \rightarrow 515.796 (5)
443.550 (3)	42.21 (25)	443.56 (4) ^a	44.40 (20)	654.9458 (23) \rightarrow 211.3624 (15)
—	—	443.70 (30) ^a	3.3 (15)	—
448.82 (9)	0.38 (15)	448.80 (20)	0.31 (15)	635.983 (25) \rightarrow 188.6796 (17)
462.354 (9)	8.1 (3)	462.34 (10)	1.60 (80)	651.132 (6) \rightarrow 188.6796 (17)
469.706 (20)	0.49 (3)	470.53 (20) ^a	0.40 (20)	758.075 (19) \rightarrow 288.2274 (21)
480.48 (3)	1.29 (15)	480.38 (8)	1.60 (10)	750.491 (15) \rightarrow 270.2069 (15)
483.713 (18)	2.19 (18)	483.61 (6)	2.60 (10)	1234.242 (6) \rightarrow 750.491 (15)
493.87 (15)	1.8 (6)	493.80 (8)	2.30 (20)	1031.75 (4) \rightarrow 537.9789 (20)
498.06 (7)	1.19 (25)	498.28 (9) ^a	0.40 (10)	767.482 (12) \rightarrow 270.2069 (15)
499.44 (13)	0.79 (12)	498.55 (13) ^a	1.40 (40)	924.05 (21) \rightarrow 425.2798 (23)
—	—	510.31 (7)	2.40 (60)	—
—	—	512.70 (20) ^a	0.50 (20)	—
515.26 (19)	5.11 (14)	515.78 (10)	1.40 (20)	515.796 (4) \rightarrow 0
527.2 (3)	1.68 (11)	527.60 (20) ^a	0.45 (12)	942.505 (20) \rightarrow 415.559 (5)
533.130 (17)	2.67 (4)	533.23 (6)	3.50 (20)	744.575 (6) \rightarrow 211.3624 (15)

Table 1 (continued)

This work Energy(keV)	I_{γ} (%)	Schneider et al. (1979) Energy(keV)	I_{γ} (%)	This work $E_i \rightarrow E_f$ (keV \rightarrow keV)
—	—	536.67 (10) ^a	1.8 (80)	—
540.513 (26)	239.11 (16)	540.49 (5)	253.6 (94)	654.9478 (23) \rightarrow 114.3534 (15)
546.22 (24)	3.85 (13)	547.13 (6) ^a	0.6 (30)	547.076 (6) \rightarrow 0
548.7 (4)	3.4 (8)	547.43 (3) ^a	0.4 (20)	758.075 (19) \rightarrow 211.3624 (15)
555.77 (3)	17.7 (13)	555.88 (9)	22.6 (12)	744.575 (6) \rightarrow 188.6796 (17)
556.71 (4)	23.9 (9)	556.83 (9)	16.8 (20)	767.482 (12) \rightarrow 211.3624 (15)
—	—	558.01 (30) ^a	2.90 (10)	—
—	—	563.79 (15) ^a	0.36 (16)	—
567.32 (14)	0.6 (3)	567.60 (20) ^a	0.64 (13)	1312.506 (20) \rightarrow 744.575 (6)
—	—	575.40 (30) ^a	0.30 (10)	—
579.17 (5)	1.2 (4)	579.28 (6)	2.90 (20)	1234.242 (6) \rightarrow 654.9478 (23)
582.144 (21)	6.26 (19)	582.92 (12) ^a	0.70 (30)	942.505 (20) \rightarrow 360.139 (5)
583.055 (13)	13.3 (4)	582.98 (8) ^a	1.90 (50)	1234.242 (6) \rightarrow 651.132 (6)
—	—	588.50 (30) ^a	0.22 (8)	—
590.74 (17)	0.16 (4)	—	—	1312.506 (20) \rightarrow 721.929 (26)
594.54 (5)	0.47 (7)	594.34 (9)	1.10 (10)	1141.67 (4) \rightarrow 547.076 (6)
598.01 (4)	0.65 (7)	598.02 (8)	1.10 (10)	785.860 (26) \rightarrow 188.6796 (17)
—	—	606.67 (16)	0.40 (20)	—
—	—	617.90 (30) ^a	0.29 (10)	—
630.225 (9)	6.01 (12)	630.23 (5)	7.30 (10)	744.575 (6) \rightarrow 114.3534 (15)
634.87 (5)	10.65 (10)	635.50 (5) ^a	2.6 (50)	750.491 (15) \rightarrow 114.3534 (15)
635.97 (4)	1.29 (12)	636.21 (11) ^a	2.0 (40)	635.983 (25) \rightarrow 0
—	—	650.97 (10) ^a	2.40 (10)	—
652.744 (7)	26.46 (15)	—	—	1190.728 (7) \rightarrow 4537.9789 (20)
654.838 (3)	276.08 (22)	654.83 (3)	307 (150)	654.9478 (23) \rightarrow 0
—	—	657.25 (12) ^a	0.7 (30)	—
660.97 (3)	1.22 (5)	661.48 (23) ^a	0.20 (8)	1411.89 (3) \rightarrow 750.491 (15)
665.22 (7)	0.59 (4)	—	—	1181.18 (6) \rightarrow 515.796 (4)
—	—	671.64 (17) ^a	0.40 (15)	—
674.38 (14)	0.40 (5)	673.59 (15)	0.42 (10)	885.82 (14) \rightarrow 211.3624 (15)
676.17 (9)	0.60 (7)	675.86 (12)	0.98 (7)	1234.242 (6) \rightarrow 556.233 (4)
681.47 (15)	0.23 (4)	681.34 (15)	0.31 (6)	1239.75 (3) \rightarrow 556.233 (4)
686.905 (16)	3.40 (21)	686.97 (4)	3.40 (20)	1234.242 (6) \rightarrow 547.076 (6)
696.191 (9)	5.60 (11)	696.26 (4)	6.6 (40)	1234.242 (6) \rightarrow 537.9789 (20)
—	—	704.07 (1)	0.13 (6)	—
712.542 (19)	2.43 (8)	712.59 (5)	2.70 (20)	924.05 (21) \rightarrow 211.3624 (15)
718.44 (4)	1.20 (6)	718.42 (9)	1.90 (20)	1234.242 (6) \rightarrow 515.796 (4)
726.822 (12)	1.54 (10)	—	—	1264.28 (5) \rightarrow 537.9789 (20)
727.23 (3)	2.55 (24)	727.87 (8)	0.63 (7)	1190.728 (7) \rightarrow 462.349 (3)
736.18 (11)	0.71 (16)	—	—	924.05 (21) \rightarrow 188.6796 (17)
740.66 (7)	0.83 (16)	740.61 (9)	0.55 (1)	1156.971 (8) \rightarrow 415.559 (5)
—	—	743.48 (39)	0.10 (4)	—
750.15 (14)	1.2 (9)	749.63 (9)	0.52 (6)	750.491 (15) \rightarrow 0
754.43 (5)	3.6 (18)	754.34 (6)	1.50 (10)	942.505 (20) \rightarrow 188.6796 (17)
759.13 (8)	3.0 (16)	758.73 (14)	0.60 (6)	758.075 (19) \rightarrow 0
762.27 (6)	0.70 (5)	761.49 (9)	1.10 (10)	1031.75 (4) \rightarrow 270.2069 (15)
—	—	765.10 (20) ^a	0.29 (29)	—
767.793 (13)	3.38 (8)	768.19 (6)	2.30 (20)	767.482 (12) \rightarrow 0
771.91 (4)	1.0 (5)	—	—	1234.242 (6) \rightarrow 462.349 (3)
775.97 (15)	0.13 (3)	774.60 (30) ^a	0.12 (5)	1411.89 (3) \rightarrow 635.983 (25)
781.32 (10)	0.20 (3)	781.33 (15)	0.15 (4)	1141.67 (4) \rightarrow 360.139 (5)
785.20 (3)	0.70 (4)	786.66 (11)	0.39 (5)	785.860 (26) \rightarrow 0
793.19 (3)	1.63 (7)	793.48 (8)	0.87 (70)	1190.728 (7) \rightarrow 396.8556 (23)
794.58 (3)	3.28 (18)	—	—	1156.971 (8) \rightarrow 360.139 (5)
—	—	796.05 (21)	0.27 (4)	—
806.10 (8)	0.97 (9)	—	—	1363.85 (4) \rightarrow 556.233 (4)
808.892 (12)	5.45 (20)	808.89 (5)	7.3 (50)	1234.242 (6) \rightarrow 425.2798 (22)

Table 1 (continued)

This work Energy(keV)	I_{γ} (%)	Schneider et al. (1979) Energy(keV)	I_{γ} (%)	This work $E_i \rightarrow E_f$ (keV \rightarrow keV)
813.09 (23)	0.28 (9)	813.07 (14)	0.44 (7)	1328.79 (9) \rightarrow 515.796 (4)
—	—	818.35 (16) ^a	0.22 (6)	—
829.81 (14)	0.71 (7)	828.66 (9) ^a	0.33 (8)	942.505 (20) \rightarrow 114.3534 (15)
832.25 (20)	0.51 (8)	832.06 (9)	0.90 (10)	1043.69 (20) \rightarrow 211.3624 (15)
835.18 (6)	1.24 (8)	—	—	1391.691 (65) \rightarrow 556.233 (4)
—	—	837.39 (8)	1.20 (10)	—
839.24 (5)	1.06 (8)	—	—	1049.655 (24) \rightarrow 211.3624 (15)
842.97 (4)	1.43 (6)	842.78 (8)	2.00 (20)	1239.75 (3) \rightarrow 396.8556 (23)
—	—	849.93 (8)	0.84 (7)	—
—	—	854.30 (30) ^a	0.17 (4)	—
858.74 (11)	0.76 (7)	—	—	1406.88 (6) \rightarrow 547.076 (6)
860.21 (3)	2.64 (19)	861.58 (8)	0.68 (7)	1049.655 (24) \rightarrow 188.6796 (17)
864.85 (11)	0.68 (26)	864.89 (20) ^a	0.51 (25)	1290.85 (22) \rightarrow 425.2798 (22)
—	—	864.90 (15) ^a	0.13 (5)	—
871.45 (6)	0.43 (9)	871.37 (7)	1.30 (10)	1141.67 (4) \rightarrow 270.2069 (15)
875.46 (14)	0.25 (9)	874.32 (25)	0.18 (40)	1234.242 (6) \rightarrow 360.139 (5)
—	—	877.92 (28) ^a	0.08 (6)	—
886.54 (16)	0.21 (9)	886.63 (20)	0.21 (4)	1312.506 (20) \rightarrow 425.2798 (22)
892.94 (9)	0.28 (4)	893.30 (10) ^a	0.17 (4)	1290.85 (22) \rightarrow 396.8556 (23)
897.09 (22)	0.11 (3)	896.65 (14)	0.15 (5)	1312.506 (20) \rightarrow 415.559 (5)
—	—	907.69 (14)	0.17 (3)	—
—	—	915.44 (19)	0.08 (4)	—
—	—	920.30 (21)	0.15 (6)	—
924.21 (10)	2.54 (16)	923.86 (6)	3.90 (30)	924.05 (21) \rightarrow 0
—	—	929.85 (35)	0.42 (5)	—
933.24 (4)	2.25 (20)	—	—	—
—	—	935.91 (13)	0.18 (3)	—
—	—	938.83 (12)	0.23 (3)	—
943.18 (21)	0.30 (13)	942.97 (17)	0.12 (4)	942.505 (20) \rightarrow 0
945.83 (14)	0.38 (15)	945.74 (8)	0.83 (7)	1234.242 (6) \rightarrow 288.2274 (21)
951.06 (18)	0.13 (7)	951.35 (20) ^a	0.10 (4)	1239.75 (3) \rightarrow 288.2274 (21)
952.61 (4)	0.39 (9)	951.85 (12) ^a	0.29 (10)	1312.506 (20) \rightarrow 360.139 (5)
964.048 (19)	2.32 (8)	963.70 (10)	0.97 (10)	1234.242 (6) \rightarrow 270.2069 (15)
968.372 (8)	7.99 (12)	967.44 (10)	0.32 (4)	1156.971 (8) \rightarrow 188.6796 (17)
—	—	972.00 (20)	0.11 (3)	—
976.2 (3)	0.25 (10)	—	—	1363.85 (4) \rightarrow 387.609 (4)
978.43 (21)	1.5 (4)	978.8 (5) ^a	0.60 (20)	1391.691 (6) \rightarrow 415.559 (5)
979.52 (22)	1.2 (3)	978.99 (7) ^a	3.00 (40)	1190.728 (7) \rightarrow 211.3624 (15)
—	—	986.70 (17)	0.09 (2)	—
992.08 (27)	0.13 (8)	992.63 (11)	0.57 (6)	1181.18 (6) \rightarrow 188.6796 (17)
993.56 (21)	0.15 (9)	994.00 (20) ^a	0.15 (7)	1264.28 (5) \rightarrow 270.2069 (15)
1016.1 (3)	0.14 (5)	—	—	1411.89 (3) \rightarrow 396.8556 (23)
1020.99 (20)	0.63 (8)	1021.85 (22) ^a	0.10 (4)	1568.63 (6) \rightarrow 547.076 (6)
1022.93 (4)	2.66 (18)	1022.79 (8) ^a	4.00 (30)	1234.242 (6) \rightarrow 211.3624 (15)
1027.6 (3)	0.12 (5)	1027.16 (11)	0.34 (6)	1141.67 (4) \rightarrow 114.3534 (15)
1031.40 (21)	0.28 (7)	1031.90 (20) ^a	0.17 (5)	1031.75 (4) \rightarrow 0
1040.7 (4)	0.21 (7)	—	—	1156.971 (8) \rightarrow 114.3534 (15)
1042.36 (17)	0.43 (15)	1041.89 (9)	1.10 (10)	1312.506 (20) \rightarrow 270.2069 (15)
1051.34 (20)	0.15 (9)	1051.90 (20) ^a	0.17 (5)	1411.89 (3) \rightarrow 360.139 (5)
1076.03 (5)	0.91 (3)	1075.97 (9)	0.80 (10)	—
1078.68 (23)	1.99 (3)	1078.77 (8)	2.44 (27)	1290.85 (22) \rightarrow 211.3624 (15)
1100.68 (3)	1.26 (26)	1100.78 (8)	1.90 (20)	1312.506 (20) \rightarrow 211.3624 (15)
1119.79 (5)	3.1 (18)	—	—	1234.242 (6) \rightarrow 114.3534 (15)
1124.62 (4)	4.2 (6)	1123.43 (18)	0.58 (9)	1312.506 (20) \rightarrow 188.6796 (17)
1125.40 (4)	2.6 (3)	1125.31 (15)	1.14 (14)	1239.75 (3) \rightarrow 114.3534 (15)
—	—	1126.6 (30)	0.12 (3)	—
—	—	1136.00 (20) ^a	0.12 (3)	—

Table 1 (continued)

This work Energy(keV)	I_γ (%)	Schneider et al. (1979) Energy(keV)	I_γ (%)	This work $E_i \rightarrow E_f$ (keV \rightarrow keV)
—	—	1141.73 (15) ^a	0.10 (4)	—
—	—	1150.04 (13)	0.09 (3)	—
—	—	1156.30 (40)	0.04 (2)	—
1170.88 (19)	0.68 (9)	—	—	1568.63 (6) \rightarrow 396.8556 (23)
1172.76 (19)	1.41 (17)	1171.74 (18)	0.15 (3)	1411.891 (32) \rightarrow 240.3946 (19)
—	—	1175.84 (12)	0.13 (3)	—
1180.54 (26)	1.53 (11)	—	—	1181.18 (6) \rightarrow 0
—	—	1190.07 (14)	0.09 (2)	—
1197.47 (19)	0.21 (4)	1197.87 (11)	0.26 (4)	1312.506 (20) \rightarrow 114.3534 (15)
1202.1 (5)	0.08 (4)	1202.20 (30)	0.06 (2)	1495.19 (11) \rightarrow 288.2274 (21)
1206.7 (3)	0.15 (6)	—	—	1495.19 (11) \rightarrow 288.2274 (21)
—	—	1225.64 (23)	0.06 (2)	—
1234.31 (5)	0.83 (8)	1234.15 (9)	1.00 (13)	1234.242 (6) \rightarrow 0
1237.61 (3)	1.49 (9)	—	—	1449.250 (23) \rightarrow 211.3624 (15)
—	—	1239.46 (30)	0.07 (2)	—
1259.22 (5)	0.048 (22)	1259.64 (13)	0.16 (3)	1449.250 (23) \rightarrow 188.6796 (17)
1263.8 (5)	0.102 (23)	1264.05 (10)	0.29 (5)	1264.28 (5) \rightarrow 0
1280.57 (6)	0.43 (3)	1280.28 (28)	0.04 (2)	1568.63 (6) \rightarrow 288.2274 (21)
—	—	1284.75 (20)	0.06 (2)	—
—	—	1290.18 (11)	0.16 (3)	—
1293.4 (4)	0.07 (3)	—	—	1293.4 (4) \rightarrow 0
—	—	1298.12 (17)	0.03 (2)	—
—	—	1307.60 (30) ^a	0.04 (2)	—
—	—	1312.20 (12)	0.28 (4)	—
—	—	1357.36 (16)	0.08 (2)	—
1367.96 (13)	0.6 (5)	—	—	1367.91 (13) \rightarrow 0
—	—	1381.33 (20)	0.08 (2)	—
1400.95 (9)	0.38 (4)	—	—	—
1407.26 (6)	0.58 (5)	—	—	1406.88 (6) \rightarrow 0
1449.56 (3)	0.32 (6)	1448.13 (44)	0.02 (00)	1449.250 (23) \rightarrow 0
—	—	1454.30 (21)	0.05 (2)	—
1495.36 (11)	0.27 (3)	1495.80 (34)	0.06 (2)	1495.19 (11) \rightarrow 0
—	—	1568.61 (35)	0.02 (1)	—

^a Deduced from coincidence data.

depopulating the level at 1190 keV, but our gate at 635 + 636 keV is consistent with this transition populating the level at 1142 keV.

According to our coincidence relationships many γ transitions could be positioned in the current decay scheme. Particularly, the peaks at 318, 449, 750, 813, 992 and 1202 keV reported previously by Firestone (1996) but not placed in the level scheme showed up in our experiment. The 241–318 keV coincidence data allowed us to interpret the 318 keV transition as depopulating the 556 level. The 449 keV transition was placed as depopulating the level at 635 keV based on the 448–189 keV coincidence relationship. The transition with energy 413 keV observed for the first time, is present in the gate at 449 keV so, this new transition was placed feeding the 635 keV, confirming placement of the 449 keV in the current decay scheme. The transition at 750 keV has been placed in the level scheme depopulat-

ing the level at 750 keV based on the 391–750 keV coincidence. The transitions at 813 and 992 keV have been placed in the proposal scheme feeding the levels at 515 and 189 keV, respectively, according to the 813–515 and 992–189 keV coincidence data. Finally, about the peak at 1202 keV, we suggest that this γ transition be placed in the present scheme depopulating the level 228 keV on the basis of the energy sum of the transitions 1202 and 288 keV.

4. Decay scheme

The level energies were obtained through a least-squares fit of the 181 transitions that could be placed in the decay scheme. The intensities that beta feed these levels were obtained from the intensity balance of transitions feeding and de-exciting the levels. The

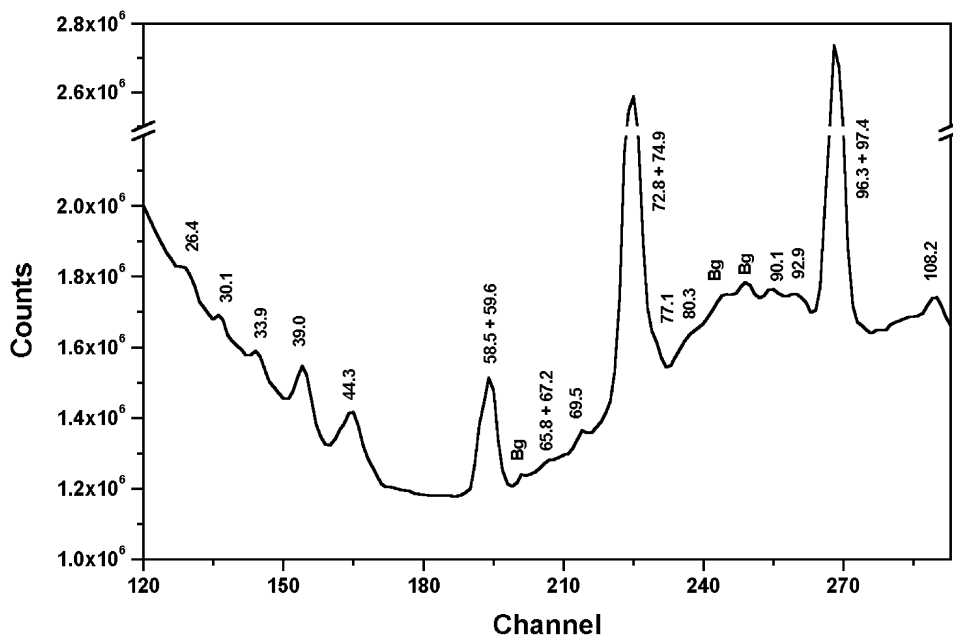


Fig. 1. Gamma-ray singles spectrum of ^{149}Nd (channel 120–300). Number above the peaks indicate energies in keV.

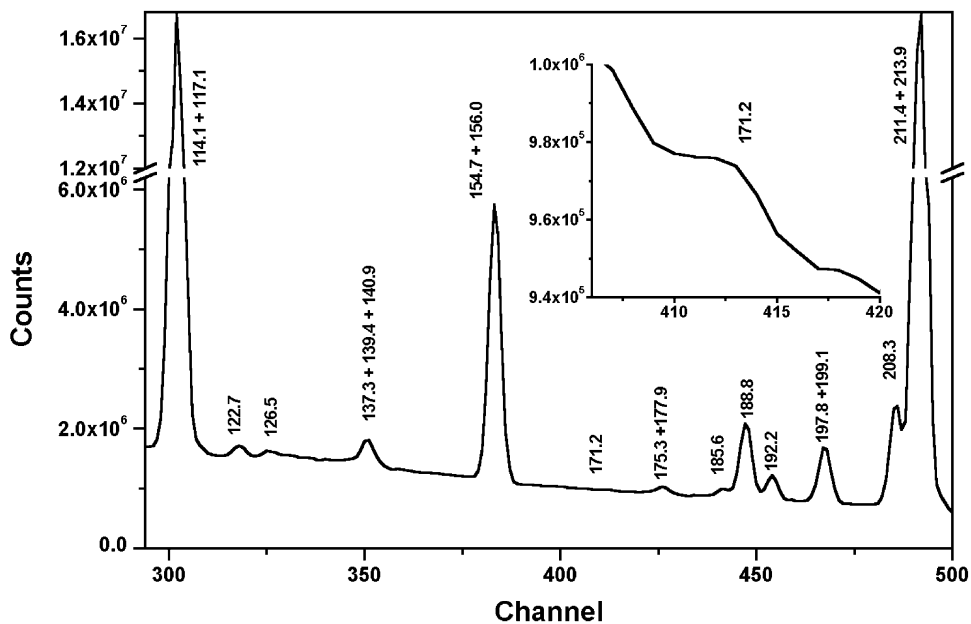


Fig. 2. Gamma-ray singles spectrum of ^{149}Nd (channel 300–500). Number above the peaks indicate energies in keV.

end-point energies were calculated from Q_{max} value reported by [Szuecs et al. \(1985\)](#). The spin assignments were based on the log ft values, calculated in the present work and on the observed decay modes.

The decay scheme consistent with these values is shown in [Figs. 11–14](#). Although the level structure of ^{149}Pm resulting from the present work differs from the schemes proposed by earlier investigations, some

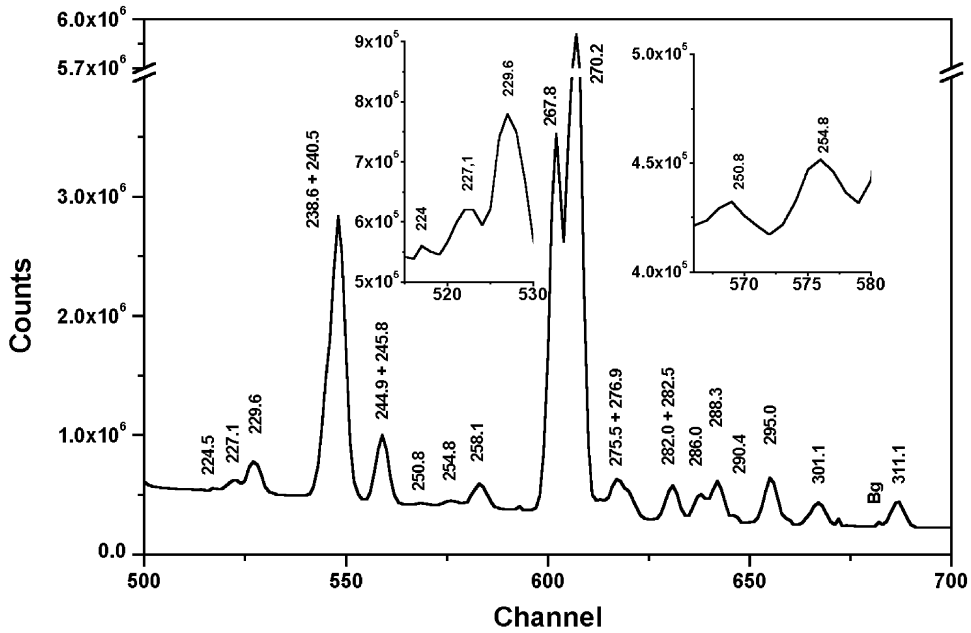


Fig. 3. Gamma-ray singles spectrum of ^{149}Nd (channel 500–700). Number above the peaks indicate energies in keV.

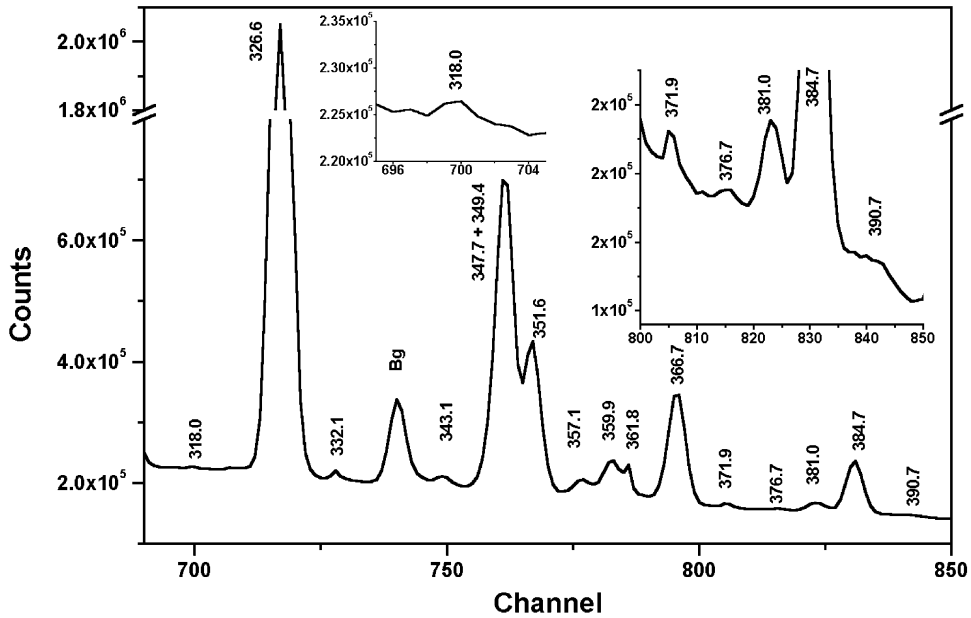


Fig. 4. Gamma-ray singles spectrum of ^{149}Nd (channel 700–850). Number above the peaks indicate energies in keV.

observed levels at ground state ($7/2^+$), 114 ($5/2^+$), 188 ($3/2^+$), 211 ($5/2^+$), 240 ($11/2^-$), 270 ($7/2^-$), 288 ($9/2^+$), 360 ($7/2^+$), 387 ($1/2^+$), 396 ($5/2^+$) and 425 keV ($7/2^+$) are already known and our results are consistent with

them. Detailed discussion about all excited levels of ^{149}Pm , which were also observed in the present study, can be found in earlier studies performed by [Chen and Arns \(1965\)](#), [Nieschimdt et al. \(1965\)](#),

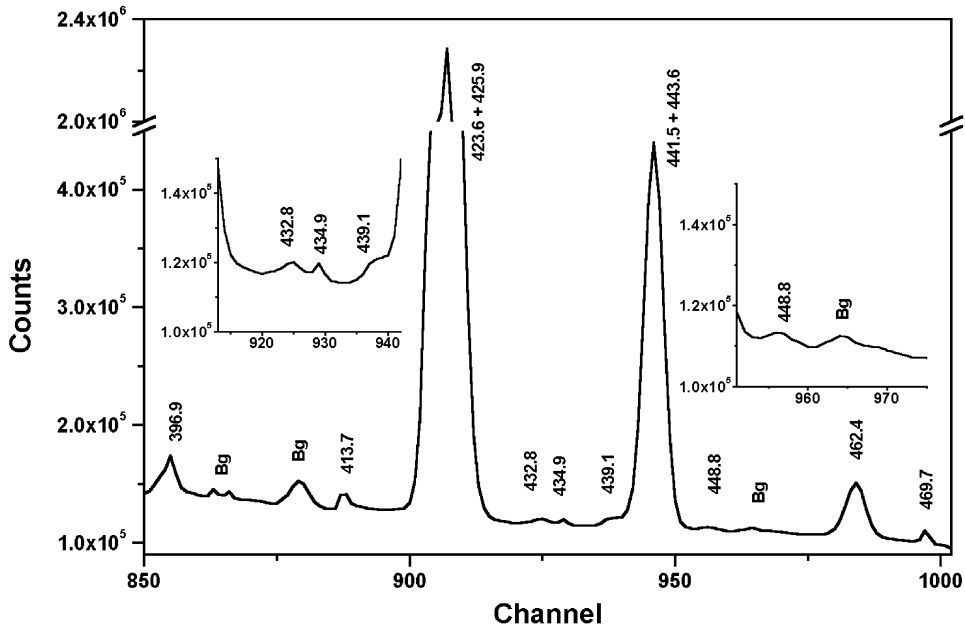


Fig. 5. Gamma-ray singles spectrum of ^{149}Nd (channel 850–1000). Number above the peaks indicate energies in keV.

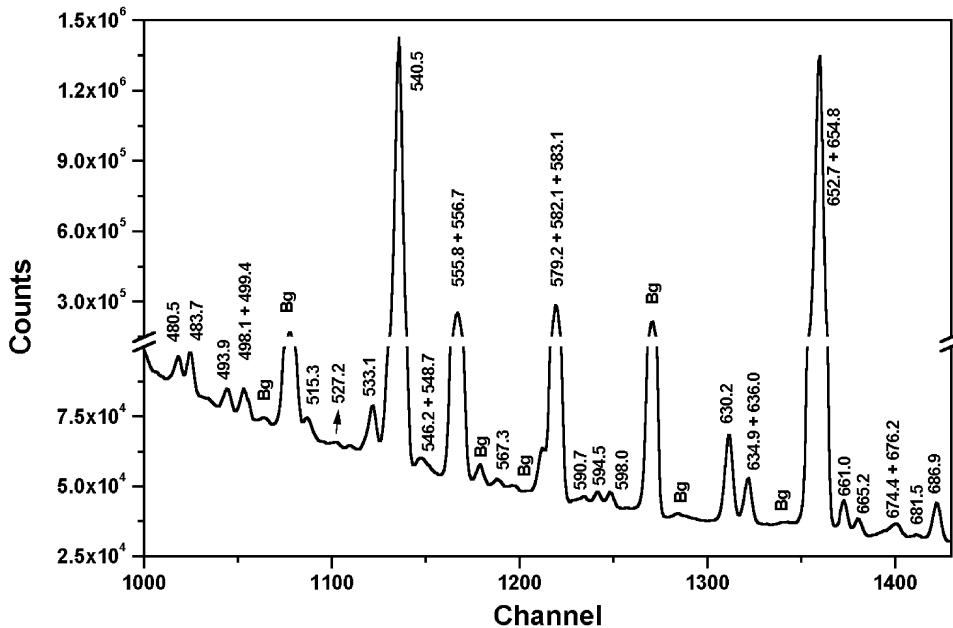


Fig. 6. Gamma-ray singles spectrum of ^{149}Nd (channel 1000–1400). Number above the peaks indicate energies in keV.

Gopinathan and Joshi (1964), Helmer and McIsaac (1966), Backlin et al. (1967), Schneider et al. (1979), Svenson et al. (1966) and also in the angular correlation measurements performed by Gopinathan

and Singru (1966), Tandon and Devare (1969) and more recently by Hideki et al. (1986). The six new excited levels proposed in this work are discussed next.

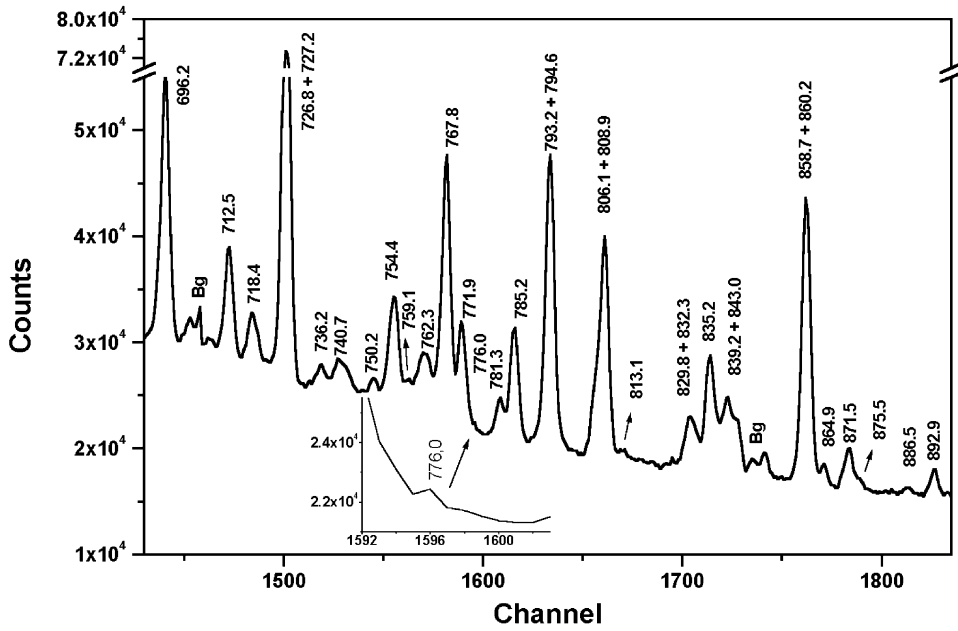


Fig. 7. Gamma-ray singles spectrum of ^{149}Nd (channel 1400–1800). Number above the peaks indicate energies in keV.

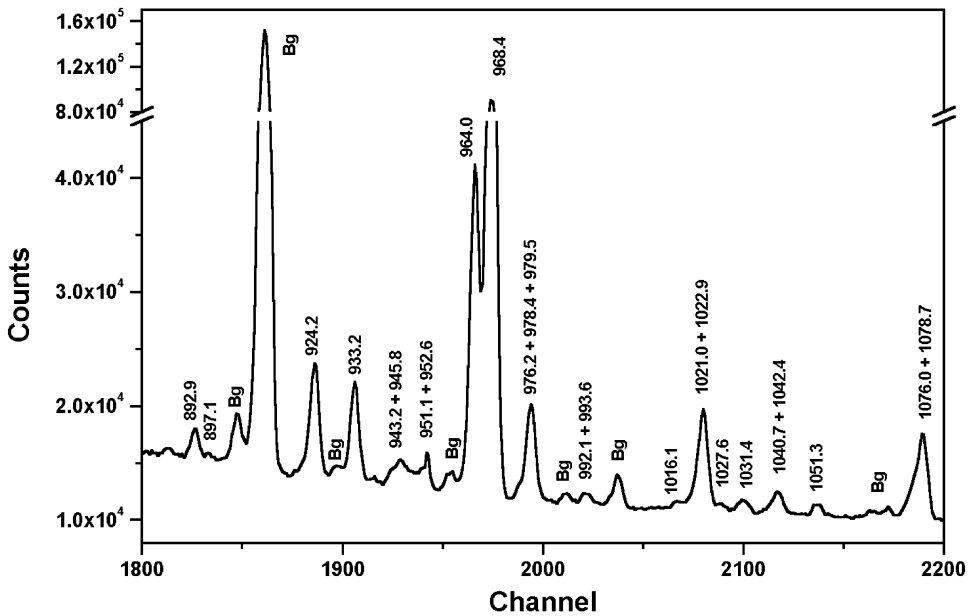


Fig. 8. Gamma-ray singles spectrum of ^{149}Nd (channel 1800–2200). Number above the peaks indicate energies in keV.

The level at 1181 keV is proposed based on the observations of the 1181 keV transition in our singles spectrum. The existence of 992–189 and 665–515 keV

coincidences is in agreement with this attribution. Further, on the basis of the 224–442 and 442–515 keV coincidences, we suggest that 224 keV transition be

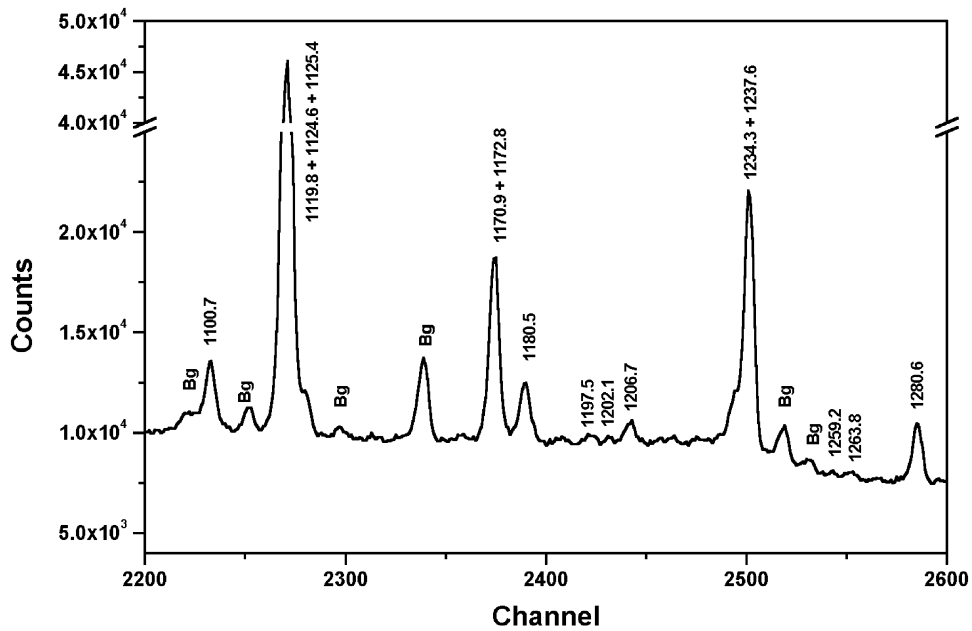


Fig. 9. Gamma-ray singles spectrum of ^{149}Nd (channel 2200–2600). Number above the peaks indicate energies in keV.

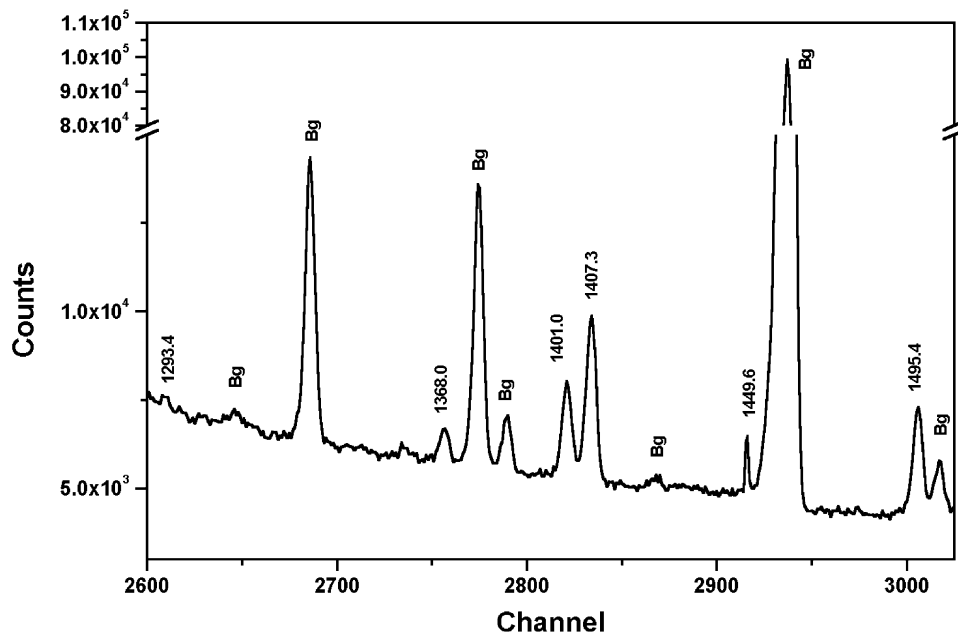


Fig. 10. Gamma-ray singles spectrum of ^{149}Nd (channel 2600–3000). Number above the peaks indicate energies in keV.

placed in the current decay scheme depopulating the new level at 1181 keV. One level with energy 1181 ± 3 keV was also observed in (^3He , d) and (α , t) nuclear reaction studies (Straume et al., 1976), in which

the assignments $3/2^+$ and $5/2^+$ were indicated. According to our coincidence data, beta feeding and log ft value, these spin assignments are consistent with our results.

Table 2
Summary of gamma–gamma coincidence in the ^{149}Nd decay

Energy (keV)	γ -rays in coincidence (keV)
39	80, 156, 199, 214
44	39, 156
60	39, 44, 192, 211, 270
67	156, 288, 541
69	97
75	44, 114 ^a , 189, 199
96 + 97	60, 77, 114, 198, 214, 268, 556
108	270, 277
114	60, 97, 123, 141, 156, 178, 189, 192, 199, 208, 214, 230, 245, 258, 276, 283, 301, 311, 327, 349 ^b , 426, 541, 556, 579, 630, 635, 687, 696, 809, 830, 843, 979, 1023, 1041, 1125
123	39, 114, 227, 301
127	156, 258, 270
137	230
139	245
141	97, 114, 126, 185, 270
156	77, 114, 127, 258, 268, 277, 381, 385, 652, 687, 696
171	327
178	114, 246
186	258
189	75, 123, 214, 227, 258, 448, 598, 696, 992, 1124
192	60, 77, 97, 114, 270
197 + 199	75, 114, 676, 806, 976
208	255, 259, 348, 583
211	60, 230, 255, 327, 444, 533, 549, 557, 696, 713, 979, 1023, 1079, 1101, 1238
214	67, 96, 114, 809
227	80, 123
230	97, 114, 246, 270, 311, 426
241	318
245	211, 241, 270
246	295
251	211
255	114, 189, 208, 283, 583
258	208, 283
268	211, 241, 270
270	245, 277, 384, 481, 498, 595, 687, 696, 865, 875, 1042
277	211, 241, 270, 595, 687
283	255, 258
286	270, 681
288	951
290	270
295	246, 270
301	332, 741, 978
311	230, 343, 499
327	211, 494, 653
343	211, 214
347 + 349	75, 114, 208, 653
357	199
367	288
377	156, 208, 655
381	114, 211, 584
385	156

Table 2 (continued)

Energy (keV)	γ -rays in coincidence (keV)
391	480, 750
397	141, 214, 230, 843, 893, 1016
424	494, 541, 655, 696
426	114, 156, 214, 230, 809, 865
442	224, 372, 515
444	211
449	188, 413
480	270, 484
484	44, 270, 480
494	114, 211, 270
498 + 499	114, 270, 311
515	442, 665, 813
541	114, 579, 655
546 + 548	211, 858
557	211
579	114, 655
583	60, 75, 114 ^b , 462 ^b , 541
598	114
630	114
635 + 636	114, 775
655	579
676	114, 246
687	114, 270, 277
696	114, 270, 327, 349, 424
713	75, 114, 211
718	276
741	301
762	270
809	246, 288, 311, 426
859	547
865	211, 270, 311
871	270
893	397
946	288
951	246
964	114, 270
994	270
1023	114
1079	211
1101	114
1125	114

^aThese coincidences can only be explained if the 75 keV transition is positioned as depopulating the level at 189 keV.

^bThese coincidences can only be explained if the 75 keV transition is positioned as depopulating the level at 462 keV. These results reinforce the suggestion that the 75 keV photopeak is an unresolved doublet.

The peak at 1293 keV is present in our singles spectra but it does not appear in coincidence with any gamma-ray. So, it is placed as a ground state transition from the 1293.4 keV level. The calculated log ft value is 8.68 which limits the spins to 3/2, 5/2 or 7/2 and positive parity.

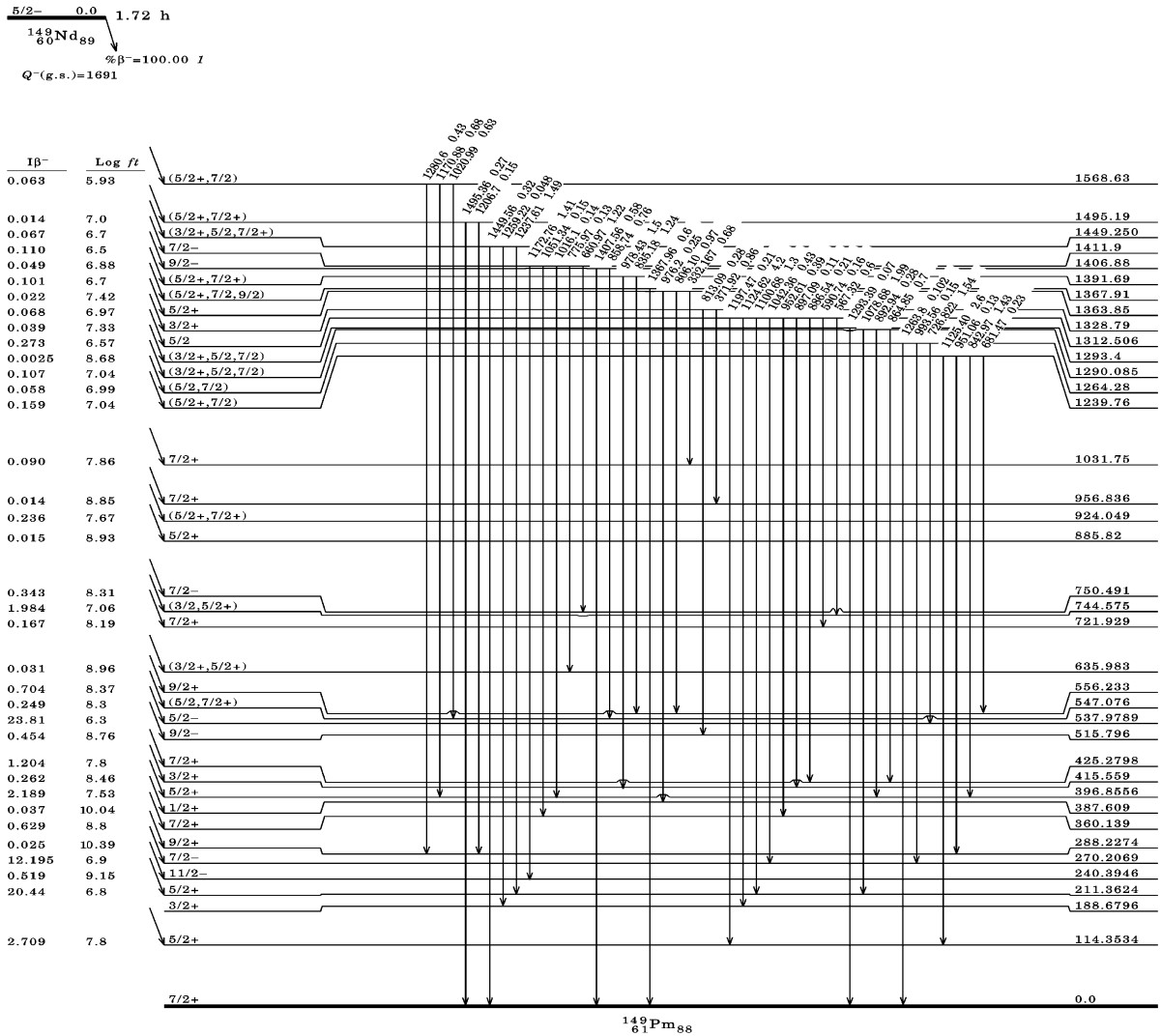


Fig. 11. Proposed level scheme for ^{149}Pm . The energies are given in keV (Part 1 of 4).

We introduce a new level at 1329 keV due to the appearance of the 813 keV gamma-ray in the coincidence data, gated by the 515 keV transition. This level was also observed in ($d,^3\text{He}$) and (α,t) nuclear reaction study (Straume et al., 1976) with energy 1329 ± 4 keV and spin and parity $3/2^+$. Our log ft value of 7.33 agrees with this assignment.

The existence of two new transitions at 806 and 976 keV, observed in our singles spectra, was confirmed based on the 806–198 and 976–199 keV coincidence relationships. The gate at 197+199 keV is consistent with the feeding of 556.2 keV ($9/2^+$) level by the 197.7 keV transition and also with the feeding of 387.6 keV level ($1/2^+$) by the 199.0 keV transition. These data are consistent with the depopulation of the new

level at 1364 keV. The introduction of this level is also supported by our energy-sum analysis. It led us to suggest that the 332 keV transition, observed for the first time, could be placed in the current decay scheme also depopulating the new level at 1364 keV to the well-known level with 1032 keV ($7/2^+$). According to this beta decay study an assignment of $5/2^+$ is favorable.

The level at 1367 ± 4 keV was established from the ^{148}Nd ($^3\text{He},d$) nuclear reaction study performed by Straume et al. (1976). It is also proposed in the present experiment based on the peak at 1368 keV observed in our singles spectra. Since this peak is not seen in coincidence with any other gamma-ray, it is placed as a transition directly to the ground state, without any gamma feeding. The parity of this level is most probably

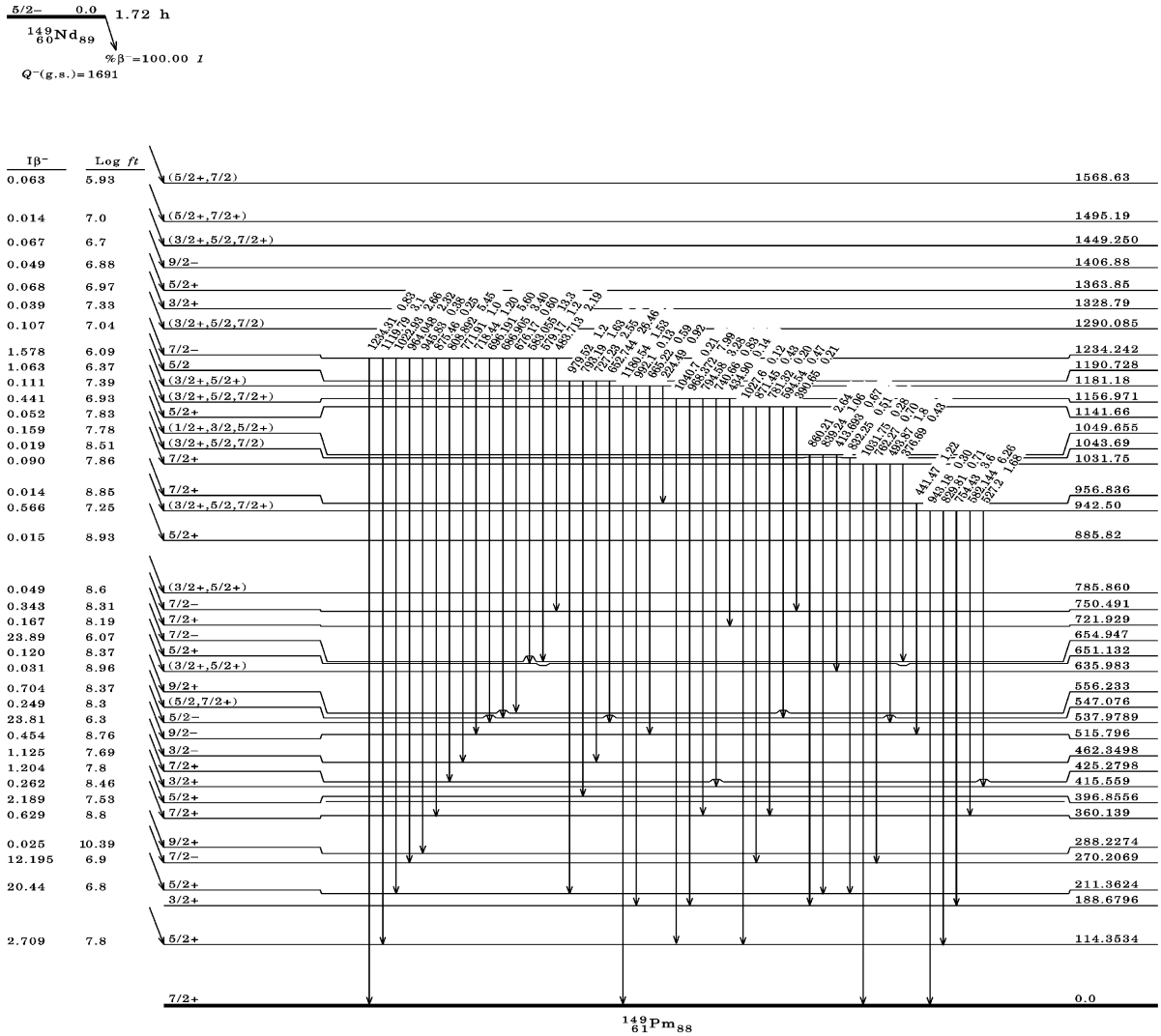


Fig. 12. Proposed level scheme for ^{149}Pm . The energies are given in keV (Part 2 of 4).

positive considering the log ft value (7.42) that limits the spins to $5/2$, $7/2$ or $9/2$.

A level with 1405 ± 3 keV energy excitation has been previously suggested by nuclear reaction study (Firestone, 1996) with a spin and parity of $9/2^-$ or $11/2^-$. In the present investigation a weak gamma-ray at 1407.3 keV was observed and placed in the current decay scheme as a ground transition from the 1406.9 keV level. Besides, the peak at 858.7 keV, observed for the first time, is also placed as depopulating this new level, based on the gate at 546 + 548 keV. The log ft value of 6.88 and the fact that this level decays to $7/2$ and $5/2$ states restricts the spin and parity assignment to $9/2^-$.

On the basis of the present results a detailed beta decay scheme of ^{149}Nd has been built where the energy and intensity of most γ transitions have been measured with better overall precision than previously. Also, using a multidetector apparatus in the coincidence experiments many multiplets could be resolved. From the 45 transitions observed for the first time, 30 have been placed into a decay scheme which includes six new levels. Besides, definite assignments of spins to the majority of excited levels in ^{149}Pm could be made. We hope these results should stimulate theoretical investigation to elucidate the extent to which susceptibility to deformation affects low-lying states of this transitional nucleus.

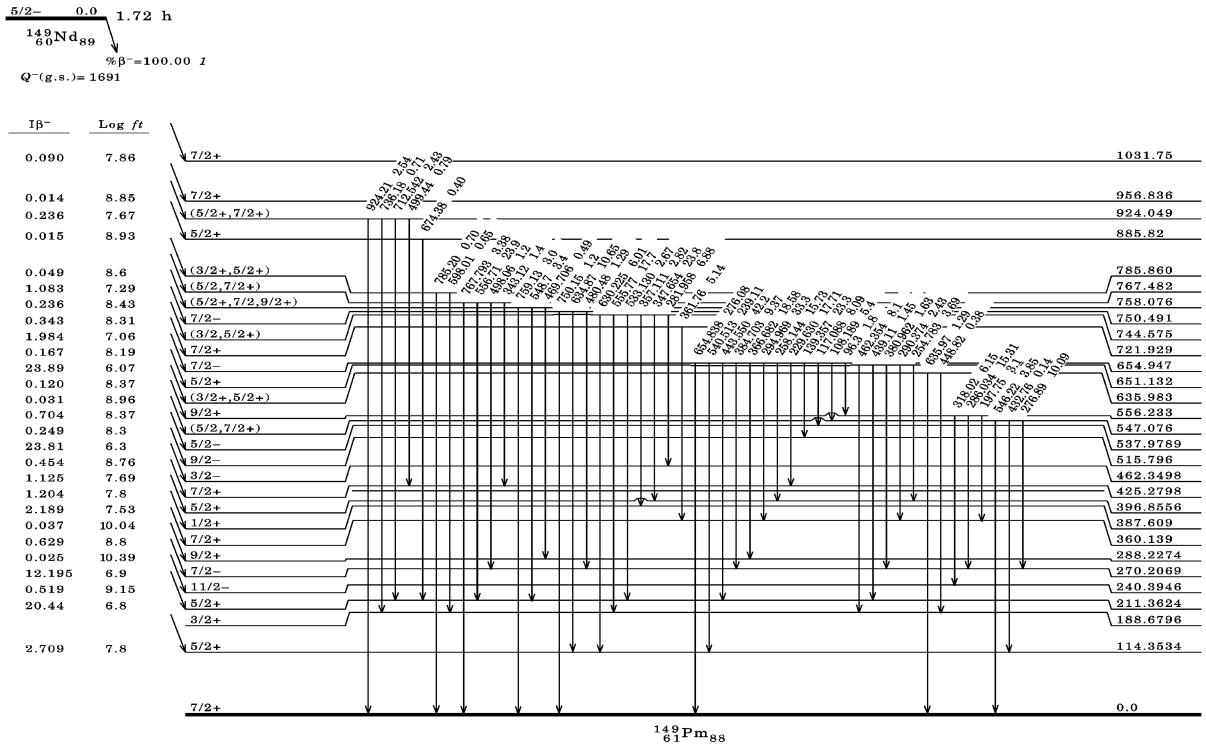


Fig. 13. Proposed level scheme for ^{149}Pm . The energies are given in keV (Part 3 of 4).

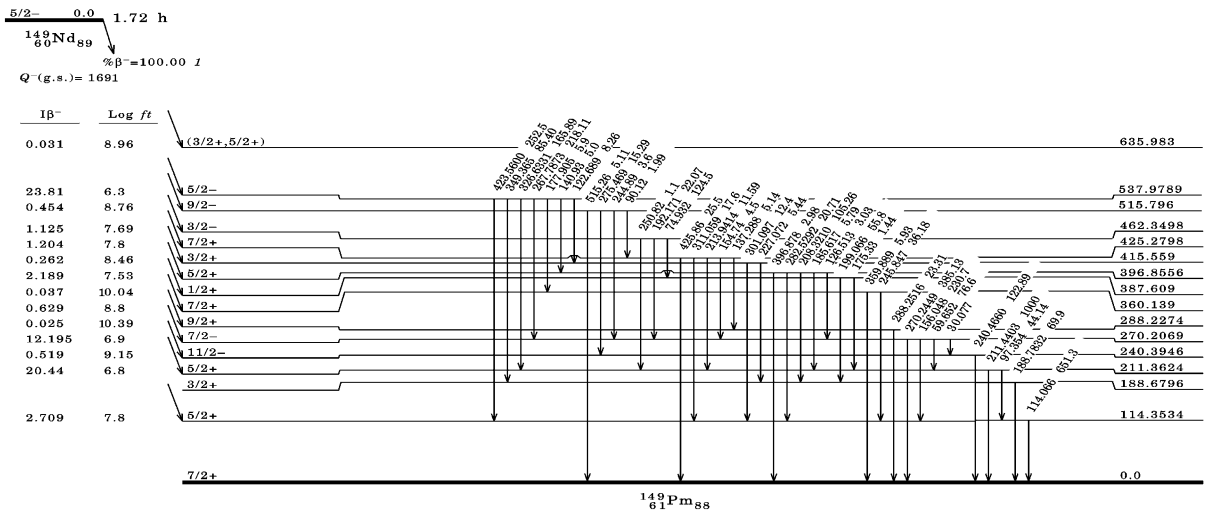


Fig. 14. Proposed level scheme for ^{149}Pm . The energies are given in keV (Part 4 of 4).

Acknowledgements

The authors would like to thank the financial support from FAPESP, CNPq and CAPES.

References

Backlin, A., Malmskog, S.G., Solhed, H., 1967. Transitions, Lifetimes and Levels in ^{149}Pm . Ark. Fys. 495–529.

- Barg, F.ºD., Neves, R.C., Vanin, V.R., 1997. Isa-to-CAMAC Interface. Proceedings of the XX Brazilian Workshop on Nuclear Physics. Guaratingueta S.P., pp. 424–426.
- Camargo, S.P., Zamboni, C.B., Medeiros, J.A.G., Kenchian, G., da Cruz, M.T.F., 1998. Decay of ^{76}As . *Appl. Radiat. Isot.* 49 (8), 997–1004.
- Chen, C.H., Arns, R.G., 1965. Energy levels of ^{149}Pm . *Nucl. Phys.* 63, 233–240.
- Firestone, R.B., 1996. Table of Isotopes, 8th Edition. New York, NY.
- Gopinathan, K.P., Joshi, M.C., 1964. Decay of ^{149}Nd to ^{149}Pm . *Phys. Rev.* 2B, 134, 297–307.
- Gopinathan, K.P., Singru, R.M., 1966. Levels of ^{149}Pm from the decay of ^{149}Nd . *Phys. Rev.* 150, 985–995.
- Guimarães Filho, Z.O., 1998. Programa BIDIM, Instituto de Física, Universidade de São Paulo, Brazil.
- Hartley, D.J., Riley, M.A., Archer, D.E., Brrown, T.B., Doring, J., Kaye, R.A., Konder, F.G., Petters, T., Pfohl, J., Sheline, R.K., Tabor, S.L., 1998. Rotational structures in ^{155}Eu and ^{157}Tb . *Phys. Rev.* C57, 2944–2961.
- Helmer, R.G., Mclsaac, L.D., 1966. Decay of ^{149}Nd . *Phys. Rev.* 143, 923–942.
- Hideki, I., Takeshi, S., Shigeru, Y., 1986. Energy levels and gamma-ray transitions in ^{149}Pm . *J. Phys. Soc. Jpn.* 55 (4), 1108–1121.
- Medeiros, J.A.G., Zamboni, C.B., Lapolli, A.L., Kenchian, G., da Cruz, M.T.F., 2001. Decay of ^{72}Ga . *Appl. Radiat. Isot.* 54, 245–259.
- Nieschmidt, E.B., Potnis, V.R., Elsworth, L.D., Mandeville, C.E., 1965. Nuclear states of ^{149}Pm . *Nucl. Phys.* 72, 236.
- Schneider, E.W., Glascock, M.D., Walters, W.B., 1979. Radioactive decay of 1.7-h ^{149}Nd to levels of transitional ^{149}Pm . *Z. Physik.* A291, 77–86.
- Straume, O., Lovhoiden, G., Burke, D.G., 1976. Proton states in $N=88$ nuclei ^{149}Pm , ^{151}Eu and ^{153}Tb populated in (TAU,D) and (ALPHA,T) reactions. *Nucl. Phys.* A266, 390–412.
- Svenson, A.G., Boston, L., Joshi, M.C., 1966. The 114 keV level in ^{149}Pm . *Nucl. Phys.* 89, 348–358.
- Szuecs, J.A., Johns, M.W., Singh, B., 1985. *Nucl. Data Sheets* for $A=149$ 46 (1), 1–185.
- Tandon, P.N., Devare, H.G.G., 1969. Factor of 114 keV state in ^{149}Pm . *Ind. J. Pure Appl. Phys.* 7, 1.